NEOPLASIA
www.neoplasia.com

Volume 13 Number 2 February 2011 pp. 180–186 180

Detection of Precursor Lesions of Pancreatic Adenocarcinoma in PET-CT in a Genetically Engineered Mouse Model of Pancreatic Cancer[1]

Volker Fendrich*, Ralph Schneider*, Anirban Maitra†,‡, Ilse D. Jacobsen§, Thomas Opfermann¶ and Detlef K. Bartsch*

*Department of Surgery, Philipps University Marburg, Marburg, Germany; †Department of Pathology, Johns Hopkins University School of Medicine, Baltimore, MD, USA; ‡The Sol Goldman Pancreatic Cancer Research Center, Johns Hopkins University School of Medicine, Baltimore, MD, USA; §Department of Microbial Pathogenicity Mechanisms, Leibniz Institute for Natural Product Research and Infection Biology – Hans Knöll Institute, Jena, Germany; ¶Department of Cell and Molecular Biology, Leibniz Institute for Natural Product Research and Infection Biology – Hans Knöll Institute, Jena, Germany

Abstract

BACKGROUND: Pancreatic cancer is among the most dismal of human malignancies. The 5-year survival rate is lower than 5%. The identification of precursor lesions would be the main step to improve this fatal outcome. One precursor lesions are called pancreatic intraepithelial neoplasia (PanIN) and are graduated in grade 1 to 3, whereas grade 3 is classified as carcinoma *in situ*. Currently, no reliable, noninvasive imaging technique (e.g., ultrasound, computed tomography, magnet resonance imaging) exists to verify PanINs. *METHODS:* Recently, a transgenic mouse model of pancreatic cancer was established in which the tumor progression of human pancreatic carcinoma is reproduced. These so-called Pdx-1 – Cre; LSL-KrasG12D/+; LSL-Trp53R172H/+ mice develop PanINs, which transform to invasive growing pancreatic carcinoma. The pancreata of mice of different ages were immunohistochemically stained using α-GLUT-2 antibodies. Furthermore, mice underwent positron emission tomography (PET)–computed tomography (CT) with ^{18}F-fluorodeoxyglucose (FDG) to evaluate early detection of PanIN lesions. *RESULTS:* An expression of GLUT-2 in murine PanINs was found in PanINs of grade 1B and higher. This finding is associated with an elevated glucose metabolism, leading to the detection of precursor lesions of pancreatic cancer in the FDG PET-CT scan. In addition, immunohistochemical staining of GLUT-2 was detectable in 45 (75%) of 60 human PanINs, whereas PanINs of grade 1B and higher showed a very extensive expression. *CONCLUSIONS:* In conclusion, we demonstrate for the first time that an elevated glucose metabolism occurs already in precursor lesions of murine and human pancreatic carcinoma. These findings are the basis for the detection of precursor lesions by PET-CT, thereby helping improving the prognosis of this devastating disease.

Neoplasia (2011) 13, 180–186

Introduction

Pancreatic cancer is a devastating and almost uniformly lethal malignancy that accounts for approximately 33,000 deaths in the United States every year, rendering it the fourth most common cause of cancer-related mortality [1]. Although the past decades have seen intense research efforts aimed at a better understanding of the underlying etiologic and pathophysiological mechanisms, this increased knowledge could not so far be translated successfully into better clinical treatment strategies and improved patient survival. In fact, during the past 30 years, the overall

Address all correspondence to: Volker Fendrich, MD, Department of Surgery Philipps University Marburg Baldingerstrasse, D-35043 Marburg, Germany.
E-mail: fendrich@med.uni-marburg.de

[1]The authors thank the National Cancer Institute's Specialized Programs of Research Excellence in GI Cancers (P50CA062924) that helped support the PanIN arrays.
Received 9 July 2010; Revised 31 October 2010; Accepted 1 November 2010

DOI 10.1593/neo.10956

median 5-year survival rates for pancreatic cancer have improved only marginally and are currently around 5% [1,2]. Notably, there is now strong evidence that invasive pancreatic adenocarcinoma proceeds through a morphologic spectrum of noninvasive ductal lesions such as pancreatic intraepithelial neoplasia (PanIN) and that histologic progression of these lesions toward invasive cancer is associated with the progressive accumulation of genetic abnormalities [2,3]. The analyses of pancreatic carcinoma have unfortunately been hampered by a number of unique challenges. For instance, at the time of diagnosis, pancreatic cancer is usually at an advanced stage and has often metastasized. The detection of these noninvasive precursor lesions would help to improve the diagnosis fundamentally. The preclinical study of PanINs has recently been made possible by the generation of genetically modified animal models, which recapitulate human PanINs and invasive pancreatic cancer on a genetic and histomorphologic level [4,5]. Now, for the first time, early detection studies or chemopreventive studies are possible [6].

In the postprandial state, increased plasma levels of glucose as well as other nutrients stimulate pancreatic β cells to secrete insulin. The initiating event in this process is the cellular uptake of glucose through the cell surface facilitative glucose transporter protein (GLUT) 2 that functions to transport glucose in proportion to circulating levels. GLUT2, also known as solute carrier family 2 (facilitated glucose transporter) member 2 (SLC2A2), is a transmembrane carrier protein that enables passive glucose movement across cell membranes and is expressed in the intestine, pancreas, kidney, and liver, which all play key roles in the handling of dietary sugars [7]. Positron emission tomography (PET) with ^{18}F-fluorodeoxyglucose (FDG) has been widely used in recent years for the diagnosis and staging of pancreatic ductal adenocarcinoma (PDAC) [8]. Indeed, FDG PET is regarded to be more accurate in the detection of primary tumors and identification of metastases than other imaging methods [9]. Despite an increasing interest in the development of specific probes for the detection of preneoplastic lesions and tumors, FDG is the most commonly applied PET strategy. The use of FDG for cancer detection relies on the increased glucose uptake associated with the exacerbated glycolytic metabolism of most malignant cells [10]. Accelerated glucose consumption can be the consequence of a variety of factors, including the overexpression of glucose transporters and hexokinases [11,12]. Recent developments using a combination of PET and computed tomography (FDG-PET-CT) have demonstrated further improvements in diagnostic sensitivity ranging from 89% to 100%. Very recently, Abasolo et al. [13] evaluated FDG PET imaging in Ela1-myc mice, a pancreatic cancer mouse model resulting in the development of tumors with either acinar or mixed acinar-ductal phenotype. They found that mixed acinar-ductal tumors could be identified several weeks before they could be palpated: Because the Ela1-myc model does not recapitulate the progression of PanIN associated with human PDAC, it was not possible to establish when—during the progression of intraductal lesions—Glut2 overexpression took place.

In this study, we show for the first time that GLUT-2 expression is detectable during an early stage of murine and human precursor lesions of pancreatic cancer. Furthermore, we demonstrate that these lesions are detectable by PET-CT in a genetically engineered mouse model of pancreatic cancer.

Materials and Methods

Mice

Conditional *LsL-Trp53^{R172H}* [14], *LsL-Kras^{G12D}*, and *Pdx1-Cre* [4] strains were interbred to obtain *LsL-Kras^{G12D};Pdx1-Cre* double mutant animals or *LsL-Kras^{G12D};LsL-Trp53^{R172H};Pdx1-Cre* triple mutant animals on a mixed 129/SvJae/C57BL/6 background as previously described [5]. All mice were generated from the same initial stock. All experiments were approved by the local committees for animal care and use. Animals were maintained in a climate-controlled room kept at 22°C, exposed to a 12:12-hour light-dark cycle, fed standard laboratory chow, and given water *ad libitum*.

Genotyping

For genotyping, genomic DNA was extracted from tail cuttings using the REDExtract-N-Amp Tissue PCR Kit (Sigma-Aldrich, St Louis, MO). Three polymerase chain reactions were carried out for each animal to test for the presence of the oncogenic Kras (using LoxP primers), p53, and Pdx1-Cre transgene constructs (using Cre-specific primers along with Gabra as a positive control), respectively.

Tissue Microarrays

Tissue samples were obtained from the pathology archives of the Johns Hopkins Medical Institutions (Baltimore, MD). PanIN tissue microarray blocks were also created as described previously [15]. In short, 60 PanIN lesions were selected from 33 patients with pancreatic ductal adenocarcinoma. PanIN lesions were separated into PanIN-1, PanIN-2, or PanIN-3 grades either at the time of microarray creation or after a review by A.M.

Histologic Evaluation

After completion of the study, mice were killed, and the pancreas was removed and inspected for grossly visible tumors and preserved in 10% formalin solution (Sigma-Aldrich) for histology. Formalin-fixed paraffin-embedded tissues were sectioned (4 μm) and stained with hematoxylin and eosin. Six sections (100 μm apart) of pancreatic tissues were histologically evaluated by an experienced gastrointestinal pathologist (A.M.). Mouse PanIN (mPanINs) lesions were classified according to histopathologic criteria as recommended elsewhere [16,17].

Immunostaining

For immunolabeling, formalin-fixed and paraffin-embedded archived tumor samples and corresponding normal tissues were stained as previously described [18]. Concentrations and sources of primary antibodies are available on request. Briefly, slides were heated to 60°C for 1 hour, deparaffinized using xylene, and hydrated by a graded series of ethanol washes. Antigen retrieval was accomplished by microwave heating in 10 mM sodium citrate buffer, pH 6.0, for 10 minutes. For immunohistochemistry, endogenous peroxidase activity was quenched by 10 minutes of incubation in 3% H_2O_2. Nonspecific binding was blocked with 10% serum. Sections were then incubated with primary antibodies overnight at 4°C. For immunohistochemistry, bound antibodies were detected using the avidin-biotin complex peroxidase method (ABC Elite Kit; Vector Labs, Burlingame, CA). Final staining was developed with the Sigma FAST DAB peroxidase substrate kit (Sigma, Deisenhofen, Germany).

FDG-PET-CT In Vivo

A Siemens Inveon small-animal multimodality PET-CT system (Preclinical Solutions, Siemens Healthcare Molecular Imaging, Knoxville, TN) was used for data acquisition. This PET-CT system is characterized by the combination of two independently operating PET and CT scanner. The PET module has an effective transaxial field of view (FOV) of approximately 10 cm and an axial FOV of 12.7 cm, whereas

radial, tangential, and axial resolution at the center of FOV is better than 1.5 mm. PET acquisitions were carried out with default settings of coincidence timing window of 3.4 nanoseconds and energy window of 350 to 650 keV. Images were reconstructed using 3D Ordered Subset-Expectation Maximization (OSEM-3D, 2 iterations, 16 subsets) algorithm followed by maximum *a posteriori* algorithm (18 iterations, 16 subsets, beta smoothing factor 0.1) (Siemens, Germany). Pixel size was 0.431 mm and slice thickness is 0.796 mm based on the size of the image matrix of 256 × 256 × 159. Attenuation was corrected based on the CT measurements. The CT module consists of a cone beam micro x-ray source (50-µm focal spot size) and a 2048 × 3072 pixel x-ray detector. Maximum FOV of the detector is 5.5 cm × 8.4 cm. Our standard micro-CT imaging protocol used 80 kV at 500 µA, 360 degrees of rotation, and 200 projections per bed position. Two bed positions were acquired with an overlap of 43.6%. Exposure time of each projection was 300 milliseconds. Micro-CT images were reconstructed using Shepp-Logan filter and cone beam–filtered back-projection (Modified Feldkamp algorithm) into 256 × 256 × 601 CT data sets with 0.217-mm voxel dimensions. Acquisitions and reconstructions were carried out using Siemens Acquisition workplace (IAW) software version 1.4.3 (Siemens).

After the CT scan was complete, the mouse bed was translated axially and centered within the PET module. The PET data were acquired 40 to 60 minutes after injection of FDG. Because the mouse remains in the same position on the bed for both CT and PET acquisitions and the relative positions of the field of views of PET and CT are known, the CT data were transformed to fuse and coregister the PET and CT data.

Visualization and analysis of the coregistered PET-CT data were performed with the Siemens Inveon Research Workplace (IRW) software version 2.2 (Siemens).

In preparation for PET-CT, mice were anesthetized with 1.5% to 2% vaporized isoflurane (DeltaSelect, Dreieich, Germany) in oxygen (1.5 l/min) to prevent animal movement and reduce imaging artifacts. During anesthesia, respiratory frequency was continuously monitored. Hypothermia was prevented by placing the mice on heating pads (36°C). ^{18}F (half-life, 109 minutes) labeled FDG (Eckert & Ziegler, Bad Berka, Germany) with an activity of 9.6 ± 0.5 MBq was injected intravenously into the lateral tail vein of anesthetized mice in a volume of 90 to 110 µl of 0.9% NaCl. Because extended fasting times may profoundly affect outcome of experimental disease in small rodents with approximately 20- to 25-g body weight and high metabolic activity, fasting was completely omitted, and mice had free access to water and food right before FDG administration and imaging.

Results

Development of PanINs in LsL-Kras^{G12D};Pdx1-Cre and of Pancreatic Cancer in LsL-Kras^{G12D};LsL-Trp53^{R172H};Pdx1-Cre Mice

As previously described in the initial reports [4,5], we observed development of low-grade (Figure 1*A*) and high-grade (Figure 1*B*) PanINs in *LsL-Kras^{G12D};Pdx1-Cre* and fully invasive pancreatic cancers (Figure 1*C*) in *LsL-Kras^{G12D};LsL-Trp53^{R172H};Pdx1-Cre* transgenic mice. The histologic diagnosis resembled ductal adenocarcinomas of the pancreas or its precursor lesions observed in humans.

Expression of Glut-2 in LsL-Kras^{G12D};LsL-Trp53^{R172H};Pdx1-Cre–Derived Murine Precursor Lesions and Pancreatic Cancer

The pancreas was harvested from *LsL-Kras^{G12D};Pdx1-Cre* and *LsL-Kras^{G12D};LsL-Trp53^{R172H};Pdx1-Cre* transgenic mice and stained for Glut-2 expression using immunohistochemistry.

In neoplastic mouse tissue, Glut-2 was expressed in 85% of all PanIN lesions graded 1B or higher (Figure 2, *A* and *B*). Whereas PanIN 1A epithelium did not show Glut-2 expression (Figure 2*A*, *arrows*), higher-graded PanIN lesions had a strong Glut-2 expression. Glut-2 expression was restricted to tumor cells, whereas the stromal compartment of the carcinoma did not show any GLUT-2 expression. These findings suggest that elevated glucose metabolism is an early event in PanIN progression and may help detect precursor lesions during a non-invasive stage. Furthermore, we found expression of Glut-2 in invasive pancreatic carcinoma (Figure 2*B*). In wild-type mice, Glut-2 expression was detected in islet cells only (Figure 2*E*).

Expression of Glut-2 in Human Precursor Lesions of Pancreatic Cancer

After the evidence of GLUT-2 expression in murine precursor lesions of pancreatic cancer at stages as early as PanIN 1B, we next sought to translate our findings into the clinics. Therefore, we evaluated a panel

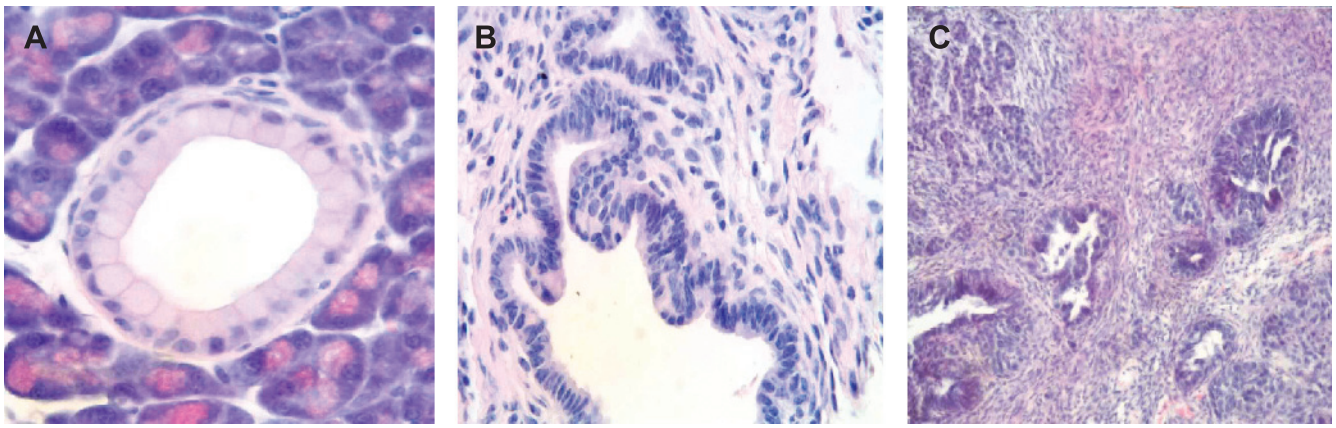

Figure 1. (A) Low-grade mPanIN lesion (mPanIN-1A) in a *LsL-Kras^{G12D}; Pdx1-Cre* mouse. (B) High-grade PanIN lesion after 5 months in a *LsL-Kras^{G12D};LsL-Trp53^{R172H};Pdx1-Cre* mouse. (C) Invasive poorly differentiated ductal adenocarcinoma from a 5-month-old *LsL-Kras^{G12D}; LsL-Trp53^{R172H};Pdx1-Cre* mouse.

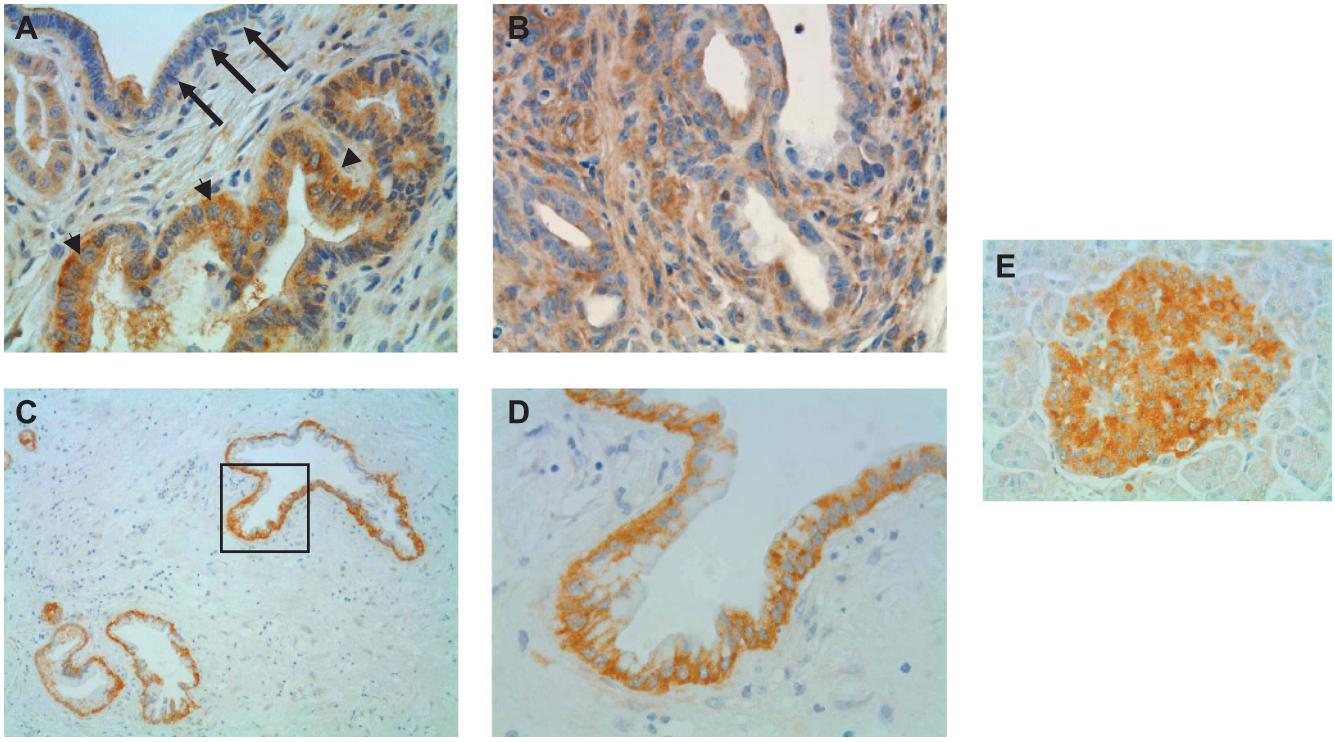

Figure 2. (A) GLUT-2 was expressed in virtually all murine PanIN lesions graded 1B or higher. PanIN 1A epithelium did not show GLUT-2 expression (arrows), and higher-graded PanIN lesions had a strong GLUT-2 expression (arrowheads). (B) GLUT-2 in invasive pancreatic carcinoma. (C, D) GLUT-2 expression was detectable in human PanIN 1B lesions (C and D). Interestingly, GLUT-2 expression was also observed only in the tumor and not in the stromal cells. (E) Normal GLUT-2 expression in islet cells.

of human PanINs by tissue microarray by GLUT-2 immunohistochemistry. Remarkably, we found the same expression pattern as in the murine counterparts. GLUT-2 expression was detectable in 45 (75%) of 60 human PanIN lesions graded 1B or higher (Figure 2, *C* and *D*). Interestingly, Glut-2 expression was also observed only in tumor but not in stromal cells (Figure 2, *C* and *D*).

Invasive Ductal Carcinomas Show High FDG Uptake in PET-CT

To determine whether FDG PET-CT could detect invasive carcinoma of *LsL-Kras^{G12D};LsL- Trp53^{R172H};Pdx1-Cre* mice, we first studied four 5-month-old transgenic mice bearing palpable tumors and age-matched nontransgenic littermates. All four control wt mice failed to display an abnormal abdominal FDG uptake in the pancreatic region (Figure 3, *A* and *D*). As expected, no tumor could be found in the pancreas of wt mice (Figure 3*G*). On the contrary, all transgenic littermates showed a strong FDG uptake in the pancreatic area (Figure 3*C*), correlating with a huge tumor burden in PET-CT scan (Figure 3*F*) and confirmed macroscopically in the abdomen of the transgenic mice (Figure 3*I*).

Precursor Lesions of Pancreatic Cancer Show FDG Uptake in PET-CT

After proving the detection and visualization of invasive pancreatic carcinoma in the *LsL- Kras^{G12D};LsL-Trp53^{R172H};Pdx1-Cre mice*, we next evaluated if it would be possible also to visualize precursor lesions of pancreatic cancer. Therefore, we analyzed four *LsL-Kras^{G12D};Pdx1-Cre* mice, which do **not** develop invasive pancreatic carcinoma but **only** PanIN lesions [4,5]. Again, we studied 5-month-old transgenic mice and age-matched nontransgenic littermates, and we were able to find a weak but clear visible signal in the pancreatic area (Figure 3, *B* and *E*). After laparotomy, no tumor was palpable or visible macroscopically (Figure 3*H*). To underline our findings, we show a series of acquired images of PET-CT in a wild-type (Figure 4*A*) and a *LsL-Kras^{G12D};Pdx1-Cre* mouse (Figure 4*B*), demonstrating that the signal was detectable throughout the series of images. According to our immunohistochemistry results, where Glut-2 expression was found only in tumor but not stromal cells, these signals arise from PanIN lesions and not from surrounding stroma or extracellular tissue.

Discussion

PET uses radiolabeled FDG, a glucose analog, to detect enhanced metabolism of glucose by malignant cells causing selective uptake of the radiotracer. FDG enters the cell through the glucose transporter protein (GLUT) transporter system and accumulates there because it is not completely metabolized. In normal pancreatic tissue, one of these transporters, GLUT2, is expressed only in pancreatic β cells [7]. PET has demonstrated efficacy in the evaluation of metastatic disease in different types cancer, such as pancreatic cancer [19]. Overall sensitivity of PET scan alone for pancreatic adenocarcinoma has been reported as 85% to 96% [20]. Although useful, the lack of anatomic localization limited the overall utility of the test. More recently, with improved computing abilities and technology, PET has been fused with CT to add precision anatomic and functional localization [20]. This colocalization has the potential benefit of improving diagnosis, staging, treatment planning, and evaluation of response to treatment in patients with pancreatic cancer. PET-CT could improve diagnosis by detection of the primary cancer. In addition, PET-CT could improve staging by identifying local regional disease and occult metastatic disease and

confirming suspicious metastatic lesions found on standard CT. Concerning the usefulness of FDG-PET in early stage pancreatic neoplasia, encouraging results have recently been reported in the diagnosis of intraductal papillary mucinous neoplasms of the pancreas with better sensitivity than conventional imaging [21].

In our study, we now show for the first time that GLUT-2 is expressed in precursor lesions of pancreatic cancer at an early noninvasive stage, making it a possible target for early detection of pancreatic cancer. This would be especially important for patients with familial pancreatic cancer that accounts for 3% to 5% of all pancreatic cancer cases [22]. Using immunohistochemistry, we found strong expression of GLUT-2 in murine PanINs grade 1B in a genetically engineered mouse model of pancreatic cancer but also in human PanINs using a tissue microarray. This shows at which stage in tumor progression of pancreatic cancer change in glucose metabolism seems to be detectable. Our results close a gap left behind by a recently published study by Abasolo et al. [13]. Using Ela1-myc mice, they showed that mixed acinar-ductal tumors could be identified by FDG PET several weeks before they could be detected by hand palpation. To gain insight into the biologic basis of the differential FDG uptake, glucose transporter expression was studied in microdissected tumor areas enriched for acinar or ductal cells. They found that GLUT2 messenger RNA levels were up to 20-fold higher in ductal than in acinar tumors. Besides, GLUT2 protein overexpression was found in ductal neoplastic cells but not in the surrounding stroma. Because the Ela1-myc model does not recapitulate the progression of PanIN progression model associated with human PDAC, it was not possible for the authors to establish when—during the progression of intraductal lesions— GLUT2 overexpression takes place. The authors stated that their work did not have direct implications regarding the early detection of pancreatic cancer in humans. However, their findings support the notion that the study of the FDG PET imaging properties of pancreatic ductal precursor lesions may contribute to develop better imaging methods to detect preneoplastic

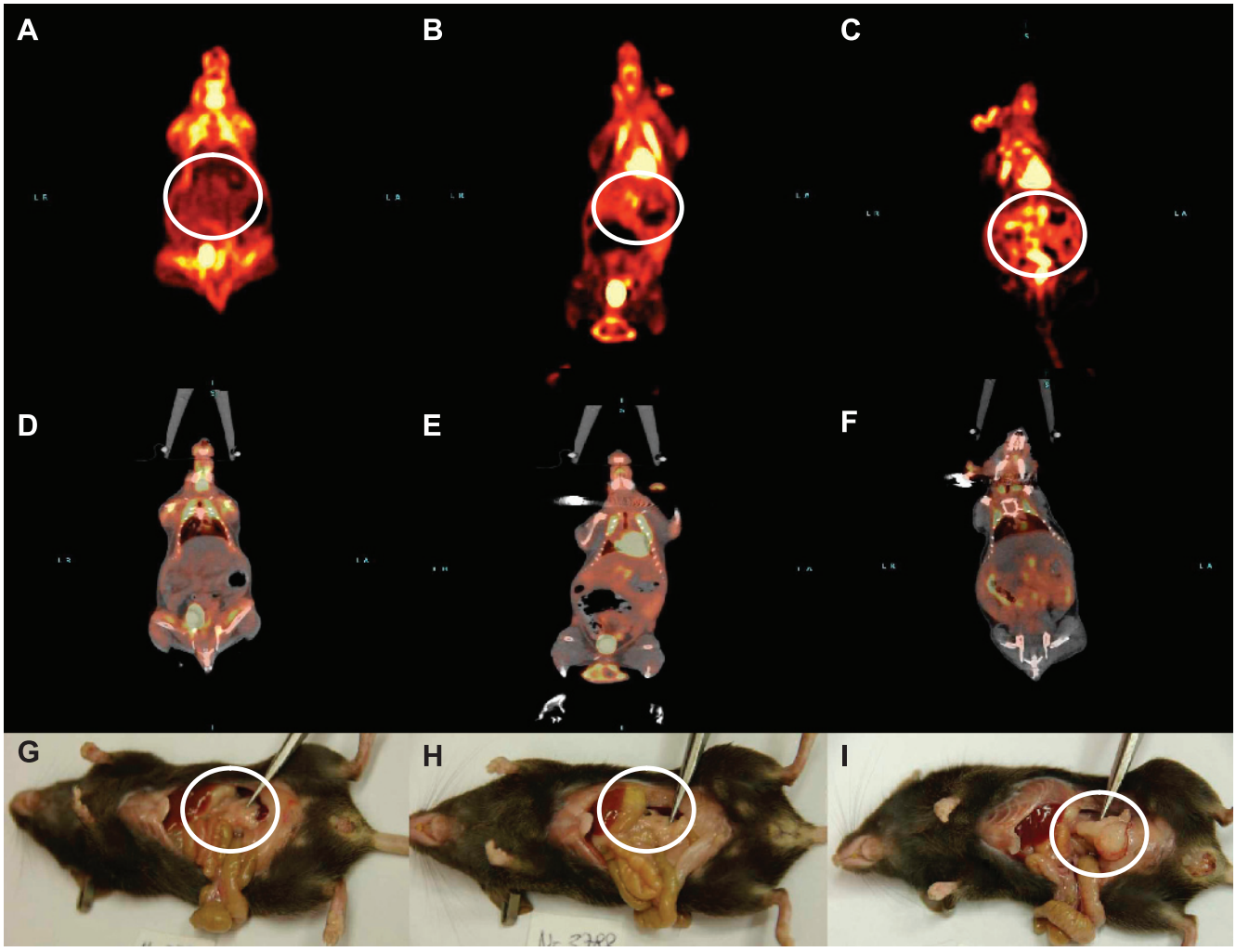

Figure 3. (A–C) PET scans. (D–F) Overlay of PET scan and CT acquired simultaneously. (E–I) Macroscopical evaluation of the pancreas and abdominal region. Pictures in one column were generated from an individual mouse. (A, D) Control wt mice displaying normal abdominal FDG uptake without enrichment in the pancreatic region (circle in A). As expected, no tumor could be found in the pancreas of the wt mice (circle in G). (B, E) *LsL-Kras^{G12D};Pdx1-Cre* mice demonstrated a weak but clear visible signal in the pancreatic area (circle in B). After laparotomy, no tumor was palpable or visible macroscopically (circle in H). (C, F) All *LsL-Kras^{G12D};LsL-Trp53^{R172H};Pdx1-Cre* littermates showed a strong FDG uptake in the pancreatic area (circle in C), which correlates to a huge tumor burden in PET-CT scan (F). As shown in I, a huge invasive pancreatic cancer was found in the abdomen of the transgenic mice (circle in I).

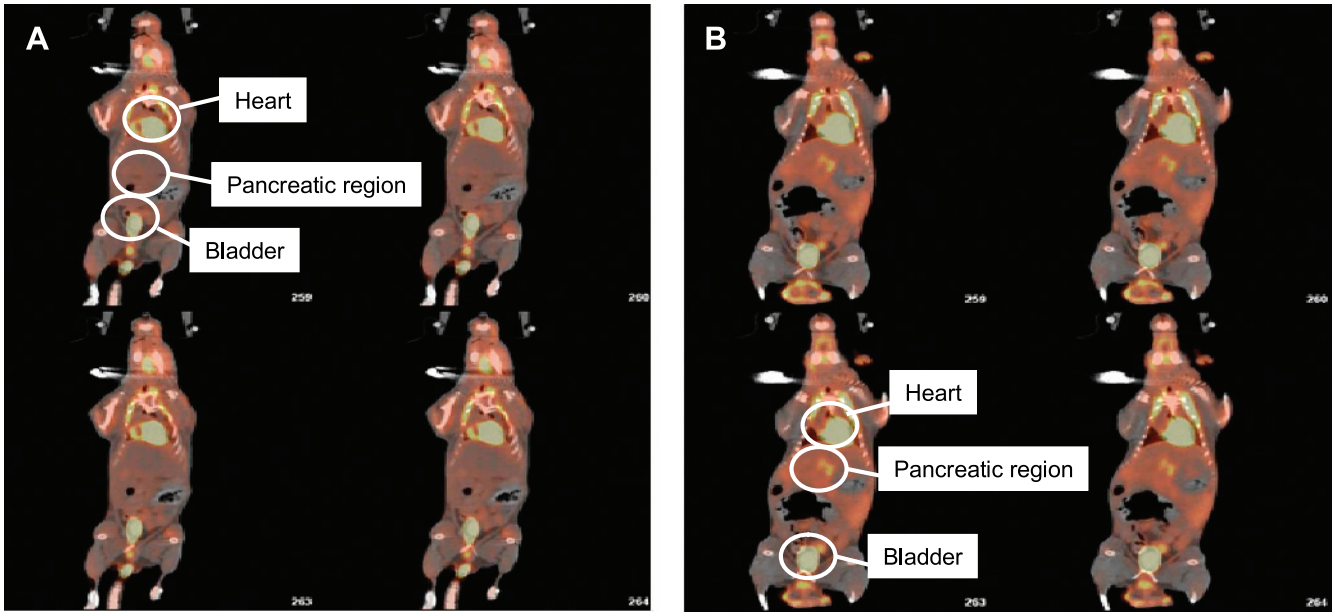

Figure 4. To underline our findings, we show a series of coronal slice images of PET-CT data in a wild-type (A) and a *LsL-Kras^{G12D};Pdx1-Cre* mouse (B), demonstrating that the signal was detectable throughout the series of slices.

lesions [13]. The conditional *LsL-Kras^{G12D};Pdx1-Cre* mice [4] used in our study is considered a very valuable tool to study PanIN biology because it mimics rather a slow progression from PanIN 1 over PanIN 2 and 3 lesions to invasive cancer in around 12 to 15 months. Furthermore, *LSL-KrasG12D/+;LSL-Trp53R172H/+;Pdx-1-Cre* [5] mice manifest widely metastatic pancreatic ductal adenocarcinoma that recapitulates the human spectrum. The use of these models now provides the opportunity to conduct chemopreventive studies on pancreatic cancer.

After we found an impressive GLUT-2 expression in 85% of murine PanINs graded 1B or higher, we stained more than 60 human PanINs from a tissue microarray for GLUT-2 and found similar expression pattern. Of 60 human PanINs, 45 (75%) revealed expression of GLUT-2, and virtually all PanINs graded 1B or higher were GLUT-2–positive. As mentioned in the study of Abasolo et al. [13], the expression was restricted to tumor cells but not to the surrounding stromal compartment.

The next step of in study was to evaluate *LsL-Kras^{G12D};Pdx1-Cre* mice, which do not develop invasive pancreatic carcinoma but develop PanIN lesions [4,5]. We studied 5-month-old transgenic mice and age-matched nontransgenic littermates and were able to find a weak but clear visible signal in the pancreatic area, whereas in wild-type mice, no such signal was detectable. Because GLUT-2 expression was restricted to neoplastic but not stromal cells, this signal is most likely based on real glucose uptake in PanIN lesions. Because only PanIN 3 are classified as carcinoma *in situ*, detecting noninvasive PanIN stages in PET-CT would have a major effect on improving the prognosis of this fatal disease and would help to detect precursor lesions in patients with familial pancreatic history in a curable stage [22]. Furthermore, we found a strong FDG uptake in the pancreatic area in *LSL-KrasG12D/+;LSL-Trp53R172H/+;Pdx-1-Cre* mice, which correlates to a huge tumor burden in the PET-CT scan, and this was verified macroscopically in the abdomen of the transgenic mice.

In conclusion, we demonstrate for the first time that an elevated glucose metabolism occurs already in precursor lesions of murine and human pancreatic carcinoma. These findings are the basis for the detection of precursor lesions by PET-CT, thereby helping improving the prognosis of this devastating disease.

References

[1] Jemal A, Siegel R, and Ward E (2006). Cancer statistics, 2006. *CA Cancer J Clin* **56**, 106–130.

[2] Feldmann G and Maitra A (2008). Molecular genetics of pancreatic ductal adenocarcinomas and recent implications for translational efforts. *J Mol Diagn* **10**, 111–122.

[3] Hruban RH, Adsay NV, Albores-Saavedra J, Compton C, Garrett ES, Goodman SN, Kern SE, Klimstra DS, Kloppel G, Longnecker DS, et al. (2001). Pancreatic intraepithelial neoplasia: a new nomenclature and classification system for pancreatic duct lesions. *Am J Surg Pathol* **25**, 579–586.

[4] Hingorani SR, Petricoin EF, Maitra A, Rajapakse V, King C, Jacobetz MA, Ross S, Conrads TP, Veenstra TD, Hitt BA, et al. (2003). Preinvasive and invasive ductal pancreatic cancer and its early detection in the mouse. *Cancer Cell* **4**, 437–450.

[5] Hingorani SR, Wang L, Multani AS, Combs C, Deramaudt TB, Hruban RH, Rustgi AK, Chang S, and Tuveson D (2005). Trp53R172H and KrasG12D cooperate to promote chromosomal instability and widely metastatic pancreatic ductal adenocarcinoma in mice. *Cancer Cell* **7**, 469–483.

[6] Fendrich V, Chen NM, Neef M, Waldmann J, Bucholz M, Feldmann G, Slater EP, Maitra A, and Bartsch DK (2010). The angiotensin-I–converting enzyme inhibitor enalapril and aspirin delay progression of pancreatic intraepithelial neoplasia and cancer formation in a genetically engineered mouse model of pancreatic cancer. *Gut* **59**, 630–637.

[7] Leturque A, Brot-Laroche E, and Le Gall M (2009). GLUT2 mutations, translocation, and receptor function in diet sugar managing. *Am J Physiol Endocrinol Metab* **296**, E985–E992.

[8] Bang S, Chung HW, Park SW, Chung JB, Yun M, Lee JD, and Song SY (2006). The clinical usefulness of 18-fluorodeoxyglucose positron emission tomography in the differential diagnosis, staging and response evaluation after concurrent chemoradiotherapy for pancreatic cancer. *J Clin Gastroenterol* **40**, 923–929.

[9] Delbeke D and Pinson CW (2004). Pancreatic tumors: role of imaging in the diagnosis, staging, and treatment. *J Hepatobiliary Pancreat Surg* **11**, 4–10.

[10] Pauwels EK, Ribeiro MJ, Stoot JH, McCready VR, Bourguignon M, and Mazière B (1998). FDG accumulation and tumor biology. *Nucl Med Biol* **25**, 317–322.

[11] Macheda ML, Rogers S, and Best JD (2005). Molecular and cellular regulation of glucose transporter (Glut) proteins in cancer. *J Cell Physiol* **202**, 654–662.

[12] Smith TA (2000). Mammalian hexokinases and their abnormal expression in cancer. *Br J Biomed Sci* **57**, 170–178.

[13] Abasolo I, Pujal J, Rabanal RM, Serafin A, Navarro P, Millán O, and Real FX (2009). FDG PET imaging of Ela1-myc mice reveals major biological differences between pancreatic acinar and ductal tumours. *Eur J Nucl Med Mol Imaging* **36**, 1156–1166.

[14] Olive KP, Tuveson DA, Ruhe ZC, Yin B, Willis NA, Bronson RT, Crowley D, and Jacks T (2004). Mutant p53 gain of function in two mouse models of Li-Fraumeni syndrome. *Cell* **119**, 847–860.

[15] Hristov AC, Cope L, Di Cello F, Reyes MD, Singh M, Hillion JA, Belton A, Joseph B, Schuldenfrei A, Iacobuzio-Donahue CA, et al. (2010). HMGA1 correlates with advanced tumor grade and decreased survival in pancreatic ductal adenocarcinoma. *Mod Pathol* **23**, 98–104.

[16] Hruban RH, Adsay NV, Albores-Saavedra J, Anver MR, Biankin AV, Boivin GP, Furth EE, Furukawa T, Klein A, Klimstra DS, et al. (2006). Pathology of genetically engineered mouse models of pancreatic exocrine cancer: consensus report and recommendations. *Cancer Res* **66**, 95–106.

[17] Hruban RH, Rustgi AK, Brentnall TA, Tempero MA, Wright CV, and Tuveson DA (2006). Pancreatic cancer in mice and man: the Penn Workshop 2004. *Cancer Res* **66**, 14–17.

[18] Fendrich V, Esni F, Garay MV, Feldmann G, Habbe N, Jensen JN, Dor Y, Stoffers D, Jensen J, Leach SD, et al. (2008). Hedgehog signaling regulates facultative progenitor activity in regenerating exocrine pancreas. *Gastroenterology* **135**, 621–631.

[19] Farma JM, Santillan AA, Melis M, Walters J, Belinc D, Chen DT, Eikman EA, and Malafa M (2008). PET/CT fusion scan enhances CT staging in patients with pancreatic neoplasms. *Ann Surg Oncol* **15**, 2465–2471.

[20] Kalra MK, Blake MA, and Saini S (2004). Role of dual PET/CT scanning in abdominal malignancies. *Cancer Imaging* **4**, 121–123.

[21] Sperti C, Bissoli S, Pasquali C, Frison L, Liessi G, Chierichetti F, and Pedrazzoli S (2007). 18-Fluorodeoxyglucose positron emission tomography enhances computed tomography diagnosis of malignant intraductal papillary mucinous neoplasms of the pancreas. *Ann Surg* **246**, 932–937.

[22] Langer P, Kann PH, Fendrich V, Habbe N, Schneider M, Sina M, Slater EP, Heverhagen JT, Gress TM, and Bartsch DK (2009). Familial pancreatic cancer—results of 5 years prospective screening of high risk individuals. *Gut* **58**, 1410–1418.